LA-5449-MS

INFORMAL REPORT



# Simulation of Turbulence in Fireballs



los alamos
scientific laboratory
of the University of California
LOS ALAMOS, NEW MEXICO 87544

UNITED STATES
ATOMIC ENERGY COMMISSION
CONTRACT W-7405-ENG. 36

In the interest of prompt distribution, this LAMS report was not edited by the Technical Information staff.

Printed in the United States of America. Available from
National Technical Information Service
U. S. Department of Commerce
5285 Port Royal Road
Springfield, Virginia 22151
Price: Printed Copy $4.00 Microfiche $1.45

LA-5449-MS
INFORMAL REPORT
UC-34
ISSUED: November 1973


# Simulation of Turbulence in Fireballs

by

Hans M. Ruppel
Richard A. Gentry
Bart J. Daly

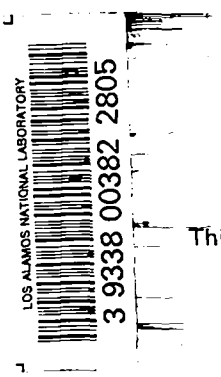


This work supported by the Defense Advanced Research Projects Agency and the Defense Nuclear Agency.

# SIMULATION OF TURBULENCE IN FIREBALLS

BY

Hans M. Ruppel, Richard A. Gentry, and Bart J. Daly

The ALE technique is applied to the calculation of a small yield, low altitude nuclear explosion. When artificial diffusion effects caused by numerical errors are minimized, the fireball rises too rapidly, reaching an altitude in excess of that which is observed. This suggests that turbulent diffusion and entrainment may be important. Hence, we have added a turbulence model to later calculations of the fireball dynamics. This report describes some of the more important features of our calculational technique and discusses the turbulence model in some detail. Preliminary results for a set of turbulence parameters and a particular low altitude fireball are presented.

---

## I. INTRODUCTION

Previous efforts to calculate the dynamics of fireballs have failed to yield a good comparison with the available data. This report discusses efforts to narrow the discrepancy between numerical simulations and empirical information. An aspect which is examined in some detail is the effect of including turbulence in the calculation.

The current work emphasizes the late time behavior (post-torus formation), when buoyancy forces and atmospheric stratification cause large fireball deformations. The primary purpose of this effort is to develop the capability to predict those aspects of atmospheric nuclear explosions that reflect on the performance of both offensive and defensive missile systems. In order to accomplish this purpose, it is necessary to determine:

(1) The size, shape, and rise rate of the fireball.

(2) The temperature, density, pressure, and velocity fields. These are particularly important for determining the effects on missiles that fly through disturbed fireball regions.

(3) The effects of turbulence. Turbulence can alter the gross behavior of the fireball via enhanced mixing, which smears out differences in temperature and density. Small-scale turbulent fluctuations are also of interest, since they can affect radar clutter return.

The initial emphasis of the LASL-DNA effort centered on the development of a new computer program, YAQUI,[1] which permits a much more accurate calculation of the mean flow hydrodynamic behavior of buoyant fireballs. The additional DARPA funding has made possible the expansion of this effort to develop a turbulence model and to incorporate this into the basic YAQUI program. This report will describe the LASL fireball turbulence modeling efforts made possible by the DARPA funds. Four aspects of our recent work are discussed.

(1) Improvements made in the basic YAQUI hydrodynamics program used to calculate turbulent fireball behavior.

(2) The turbulence model equations used to compute the turbulence field.

(3) The parameters that must be determined to complete the turbulence model.

(4) The effects of turbulence on fireball behavior as indicated by some preliminary calculations.

## II. THE BASIC HYDRODYNAMICS PROGRAM

In the present model the turbulence field generated in a fireball is completely determined by the properties of the mean flow-field. Thus, no attempt to implement the turbulence model can be successful unless the dynamics of the mean flow is faithfully represented. This implies that the development and incorporation of a turbulence model into the YAQUI fireball dynamics program must include a careful treatment of the nonturbulent hydrodynamics.

The YAQUI code used in this study is a modified version of the ALE technique[2] for hydrodynamic studies. This technique is well qualified for fireball calculations, since it permits great flexibility in mesh resolution and mesh motion. In the early, developmental stages of this method, the calculational grid consisted of rectangular cells of variable size: small cells for high resolution in the active regions of the fireball and much larger cells in the peripheral areas. Although it was possible to maintain sharp temperature gradients to late time with this resolution, a discrepancy between the calculated and the observed rise history existed. To reduce this discrepancy, a Lagrangian-like rezone[3] procedure was incorporated. This improved the comparison of rise rate with experiment. The reason for this improvement is that the rezone procedure minimizes the relative motion of the grid and the fluid, and hence reduces the diffusive truncation errors inherent in the convection process.[4]

The grid is moved according to

$$\vec{X}^{n+1}_{i,j} = \vec{X}^{n}_{i,j} + \vec{U}^{L}_{i,j}\,\delta t + f\,(\vec{X}^{n}_{i,j} - \langle \vec{X}^{n} \rangle)\ ,$$

where $\vec{X}^{n}_{i,j}$ is the radius vector at time level n, $\vec{U}^{L}_{i,j}$ is the fluid velocity of vertex (i,j), f is a variable relaxation coefficient, and $\langle \vec{X}^{n} \rangle$ is the average value of the coordinates of the four cell vertices nearest to $\vec{X}^{n}_{i,j}$. Figure 1 displays a typical mesh at a time of 15 sec juxtaposed with a plot of the temperature contours.

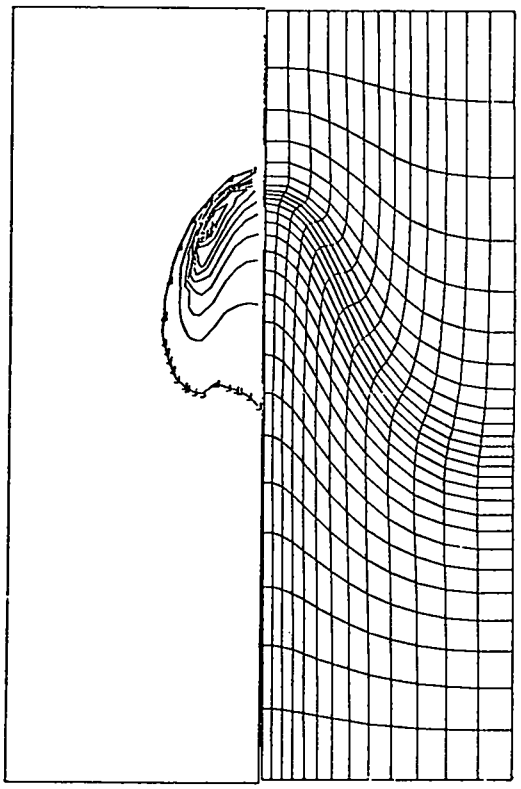

Fig. 1. Juxtaposition of Lagrangian-like calculation mesh with contours of isotherms at 15 sec after burst for a typical fireball.

This figure illustrates the manner in which the mesh lines follow the contours and the smaller cells collect in the region of large gradients. The correspondence among grid lines and temperature and density contours implies a minimal flux of fluid and heat through the cells and hence a relatively nondiffusive calculation. The reason for this is that the diffusion in the convective phase is proportional not only to the gradient of the quantity being convected but also to the relative velocity of grid and fluid and the cell dimension in the direction of the relative velocity. As is evident in Fig. 1, the present rezoning algorithm allows small cells to follow the region of maximum temperature gradient while holding the fluxing velocity to a minimum.

## III. THE TURBULENCE MODEL

To model the effects of turbulence, we have adopted the turbulence transport approach of Daly and Harlow.[5] With this representation, the contribution of turbulence to mean flow dynamics appears in the form of second-order moments of fluctuating quantities in the conservation equations of fluid flow. Some means must be provided for interpreting these second-order correlations in order to close the system of equations. The approach used has been to derive transport equations for these correlations directly from the fluctuating momentum equations. Approximations are introduced for the higher-order moments that appear in these equations, and then the entire system of equations, for mean and fluctuating quantities, is solved simultaneously.

Begin by assuming that all of the flow variables can be written as the sum of mean and fluctuating parts, thus:

$$\rho = \bar{\rho} + \rho' \ , \qquad \text{(density)} \qquad (1)$$

$$u_i = \bar{u}_i + u_i' \ , \qquad \text{(velocity)} \qquad (2)$$

$$\rho I = \overline{\rho I} + (\rho I)' \ , \qquad \text{(internal energy)}, \qquad (3)$$

where the overbar indicates an ensemble average. The ensemble average of a single fluctuating quantity will vanish by definition but the average of products of fluctuating quantities will, in general, not vanish. Thus,

$$\overline{u_i'} = 0 \ , \ \overline{u_i' u_j'} \neq 0 \ , \text{ etc.},$$

The expressions (1) - (3) are substituted into the conservation equations and these equations averaged to give:

mass equation -

$$\frac{\partial \bar{\rho}}{\partial t} + \frac{\partial}{\partial x_j} \left( \bar{\rho}\, \bar{u}_j + \overline{\rho' u_j'} \right) = 0 \qquad (4)$$

momentum equation -

$$\frac{\partial}{\partial t} \left( \bar{\rho}\, \bar{u}_i + \overline{\rho' u_i'} \right) + \frac{\partial}{\partial x_j} \left( \bar{\rho}\, \bar{u}_i\, \bar{u}_j + \bar{u}_i\, \overline{\rho' u_j'} + \bar{u}_j\, \overline{\rho' u_i'} + \overline{\rho u_i' u_j'} \right) = \frac{\partial \bar{p}_{ij}}{\partial x_j} + \bar{\rho}\, g_i \ , \qquad (5)$$

internal energy equation -

$$\frac{\partial}{\partial t} \overline{\rho I} + \frac{\partial}{\partial x_j} \left( \overline{\rho I}\, \bar{u}_j + \overline{\rho u_j' I'} \right) = \bar{p}_{ij} \frac{\partial \bar{u}_i}{\partial x_j} + \overline{p_{ij}' \frac{\partial u_i'}{\partial x_j}} \ , \qquad (6)$$

where

$$p_{ij} = - p\, \delta_{ij} + \frac{1}{2} \lambda\, e_{\ell\ell}\, \delta_{ij} + \mu\, e_{ij} \ , \qquad (7)$$

and

$$\delta_{ij} = \begin{cases} 1 & i = j \\ 0 & i \neq j \end{cases} \ ,$$

$$e_{ij} = \frac{\partial \bar{u}_i}{\partial x_j} + \frac{\partial \bar{u}_i}{\partial x_i} \ .$$

In the above, $\mu$ and $\lambda$ are the first and second coefficients of viscosity.

The goal of this research has been to obtain a turbulence representation that is universal in applicability; indeed these equations have been applied with success to a variety of turbulent flow studies. Generally, these studies have required the solution of transport equations for all components of the Reynolds stress, $\overline{\rho u_i' u_j'}$ (except those that would tend to vanish due to problem symmetries) as well as for the turbulence energy dissipation rate, $\frac{1}{2} \overline{\left( \frac{\partial u_i'}{\partial x_j} \right)^2}$. The solution of such a large set of complicated equations is very time-consuming, so that in engineering applications one would hope to make use of the experience gained in these studies while confining his attention to a simpler system of equations. In the fireball study the turbulence representation is obtained from the solution of a single transport equation for the turbulence energy, $\rho q$, together with a specified scale, s, of the energy-carrying turbulent eddies. In the following section we show how the turbulence energy equation is derived and how the effects of turbulence are incorporated into the mean flow equations.

The turbulence energy per unit volume is defined by the relationship,

$$\bar{\rho} q = \frac{1}{2} \overline{\rho\, u_\ell' u_\ell'} \ , \qquad (8)$$

while the generalized Reynolds stress tensor, $R_{ij}$, is approximated by

$$\overline{\rho u_i' u_j'} = \left(\frac{2}{3} q + \frac{1}{3} \sigma \overline{e_{\ell\ell}}\right) \bar{\rho}\, \delta_{ij} - \sigma \bar{\rho}\, \overline{e_{ij}}, \qquad (9)$$

where $\sigma = \sigma(q,s)$ is the turbulent kinematic viscosity. Notice that, on contraction of indices, Eq. (9) reduces to Eq. (8).

Various moments of fluctuating quantities appear in Eqs. (4), (5) and (6). In approximating these terms, we will make extensive use of the scalar flux approximation,[5]

$$\overline{Q' u_i'} = - \sigma \frac{\partial \bar{Q}}{\partial x_i} \quad , \qquad (10)$$

where Q is any scalar quantity. Using this approximation and dropping the overbars, we can write the basic equations to describe the mean flow and the turbulence as:

mass equation -

$$\frac{\partial \rho}{\partial t} + \frac{\partial}{\partial x_j}\left(\rho u_j\right) = \frac{\partial}{\partial x_j}\left(\sigma \frac{\partial \rho}{\partial x_j}\right)$$

momentum equation -

$$\frac{\partial}{\partial t}\left(\rho u_i\right) - \frac{\partial}{\partial t}\left(\sigma \frac{\partial \rho}{\partial x_i}\right) + \frac{\partial}{\partial x_j}\left(\rho u_i u_j\right) = \rho g_i + \frac{\partial}{\partial x_j}\left[p_{ij} - \frac{2}{3}\rho\left(q + \frac{1}{2}\sigma e_{kk}\right)\delta_{ij} + \rho\sigma e_{ij} + \sigma\left(u_i \frac{\partial \rho}{\partial x_j} + u_j \frac{\partial \rho}{\partial x_i}\right)\right] \quad ,$$

internal energy equation -

$$\frac{\partial \rho I}{\partial t} + \frac{\partial \rho u_j I}{\partial x_j} = p_{ij} \frac{\partial u_i}{\partial x_j} + \frac{100 \rho \sigma q}{s^2} + \frac{\partial}{\partial x_j}\left(\sigma \frac{\partial \rho I}{\partial x_j}\right) \quad ,$$

turbulence energy equation -

$$\frac{\partial \rho q}{\partial t} + \frac{\partial}{\partial x_i}\left(\rho u_i q\right) = - \frac{\sigma}{\rho} \frac{\partial \rho}{\partial x_i} \frac{\partial p}{\partial x_i} + \rho\sigma e_{ij} \frac{\partial u_j}{\partial x_i} + \frac{\partial}{\partial x_i} \sigma \frac{\partial \rho q}{\partial x_j} - \frac{1}{3} \rho e_{kk}\left(q + \frac{1}{2}\sigma e_{\ell\ell}\right) - \frac{100 \rho \sigma q}{s^2} \quad .$$

In the above

$$\sigma = 0.02 s \sqrt{2q} \quad .$$

A detailed list of the symbols used is included in App. A.

An assumption which is made in the derivation of this model is that there exists a state of equilibrium among eddies of all sizes. We assume, in other words, that the time taken to equilibrate the cascade process, by which energy is transferred from the largest eddies where it is created to the smallest eddies where it is dissipated, is small compared to the times that matter in the problem. Current estimates for this equilibration time in fireballs vary from perhaps one-tenth to one torus formation time, but these numbers are uncertain.

## IV. PARAMETERS OF THE MODEL

In calculations with this model, it is necessary to estimate the size of the integral scale; that is, the size of the energy-carrying turbulent eddies. We use a phenomenological form fitted to the experiments of Wygnanski and Fiedler,[6] who measured the scale and the mean and fluctuating velocity profiles in turbulent free jets. We fit their data with the expression,

$$s(r,z) = 0.14\, d(z) \begin{cases} 2 - \dfrac{v(r,z)}{v(0,z)} \, , & v(r,z) > 0 \\ 2, & v(r,z) \le 0 \end{cases} \quad ,$$

where d(z) is the radial distance at a given z from the axis to the point at which the vertical component of velocity, v(r,z), changes sign. This is approximately the radius to the point of maximum amplitude of vorticity. The scale has its minimum on the axis and rises to a maximum where v(r,z) vanishes. Its magnitude varies from perhaps 1/20th to 1/5th km over the fireball. An alternative to this empirical approach is the use of a transport equation for the decay tensor, $D_{ij}$.

Figures 2 and 3 give an indication of the effect of the scale on the turbulence energy. These figures show the variation with time of the maximum and total turbulence energy, respectively. In both cases the dashed curve was calculated with a constant scale, s = 0.1 km while the solid curve was obtained with a simplified version of the phenomenological scale discussed above.

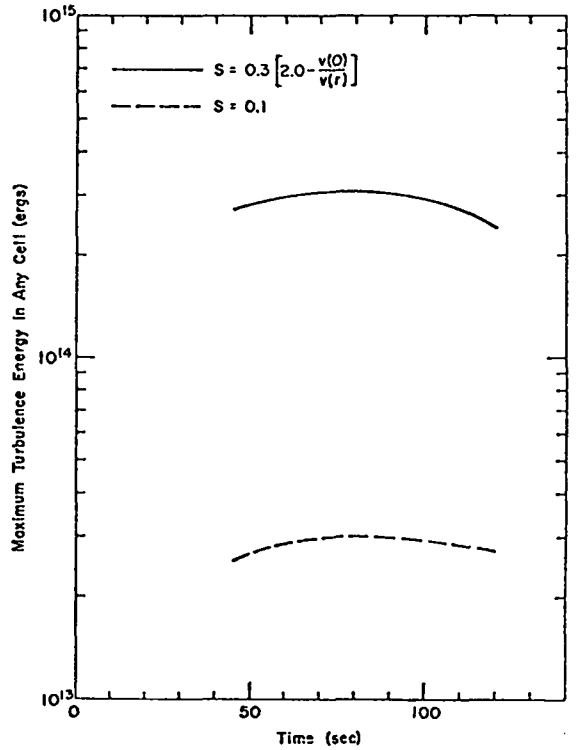


Fig. 2. Maximum turbulence energy in calculations with two different integral scale expressions.

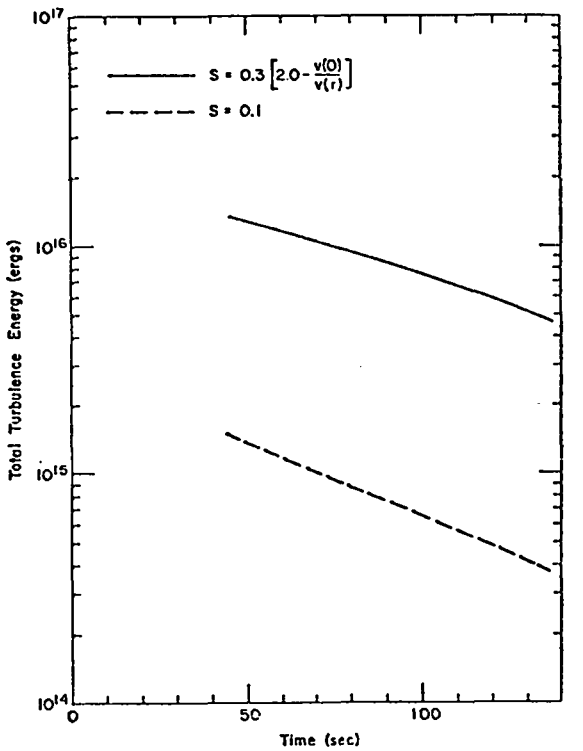


Fig. 3. Total turbulence energy obtained in calculations with different integral scale expressions.

The scales differ by about a factor of 3 and the energies by roughly an order of magnitude. One can argue that this is a consistent picture by equating the creation and decay at steady state. Since the creation is proportional to $\sigma$ X mean flow quantities and the decay is proportional to $\sigma q/s^2$, one has

$$\sigma A = \sigma B q/s^2 \quad ,$$

where A and B are combinations of constants and mean flow quantities. If then the mean flow is roughly independent of the scale, this results in

$$q \sim s^2 \quad .$$

This argument is to be taken only as an indication of the order of the effect of the scale on the turbulence energy. In the phenomenological scale calculation shown in Fig. 3, the total turbulence energy is about 1% of the total kinetic energy of the flow.

It is interesting to note that the rise altitude, as defined by the position of the cell with the maximum internal energy, is little affected by changes in the scale. Figure 4 displays the altitude as a function of time for two scale expressions. The x's were obtained with a scale 50% larger than those of the solid curve. Yet, at 210 sec there is only a 1/2 km difference in height. There appears to be no difference in the two calculations for times less than 75 sec. Indeed, this last point has been a consistent finding in all of our calculations. We find that the turbulence has virtually no effect on dimensional data at less than 75 sec and only a slight effect thereafter. This conclusion may depend on the expression for $\sigma$ that we are using, but nevertheless seems to indicate quite strongly that the effects of turbulence on the overall dynamics are relatively slight, within apparently reasonable ranges of the parameters involved.

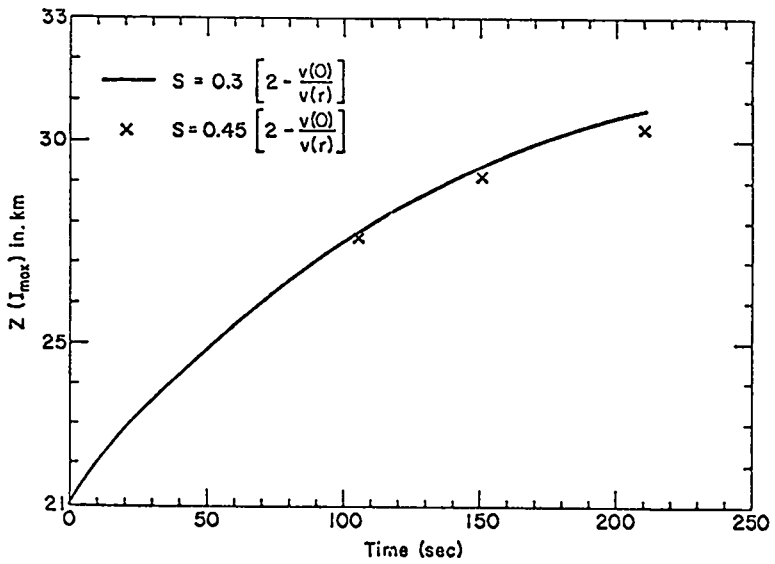


Fig. 4. Altitude as a function of time for two scales, one 50% larger than the other.

Although there is general agreement in models of this type that $\sigma$ may be expressed as $\sigma = \beta s\sqrt{2q}$, the values of $\beta$ differ among the various investigators. We currently use a value of $\beta = 0.02$, which value is based on the work of Launder, Morse, Rodi, and Spalding.[7] They compared six turbulence models in the prediction of free shear flows. In the model that they call the Prandtl energy model, they define a turbulence viscosity that is analogous to the above expression for $\sigma$ and in comparison with experiment they arrive at the value for $\beta$ that we are currently using. We then performed an independent check by testing this result against the channel flow studies of Laufer,[8] and found that a value of $\beta = 0.02$ produced good agreement between the turbulence model and the experimental measurements.

Another point that must be addressed is the seeding of the initial turbulence. From the equation for the turbulence energy it is clear that in order to generate turbulence, it is necessary that some turbulence be already present. In the real fireball, hydrodynamic instabilities may serve to initiate the turbulence. In our numerical simulations, we must seed the turbulence in some appropriate way. Figure 5 demonstrates that the magnitude and distribution of turbulence at late time is essentially independent of the method and level of seeding. Contour plots of the turbulence energy are displayed for two rather different seedings: In the upper plots the seeded turbulence was proportional to the mean flow vorticity field, while in the lower plots it was proportional to the mean kinetic energy at the same time. Clearly the two methods of seeding yield marked differences in level and configuration initially, but by 30 sec they have coalesced into a single distribution. What has happened is that the turbulence has decayed away in regions that cannot support it and has grown in those placed where shear and buoyancy create it.

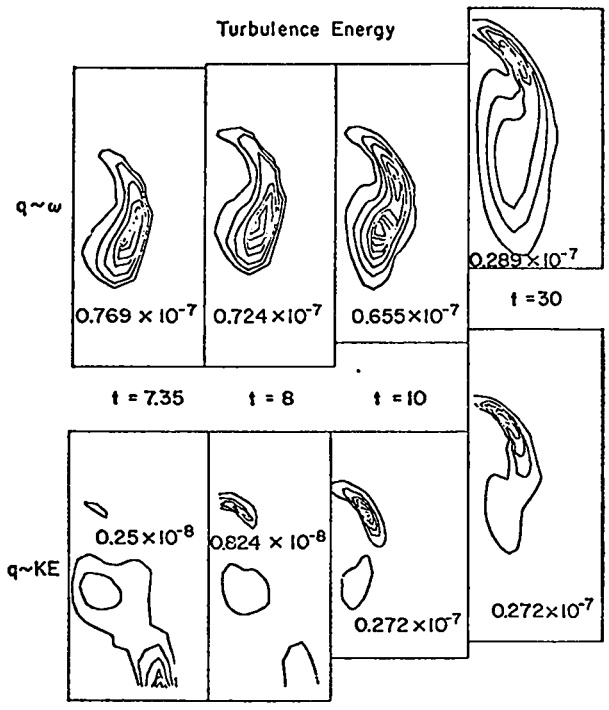


Fig. 5. Turbulence energy contours and maximum turbulence energy for four times with two different initial distributions.

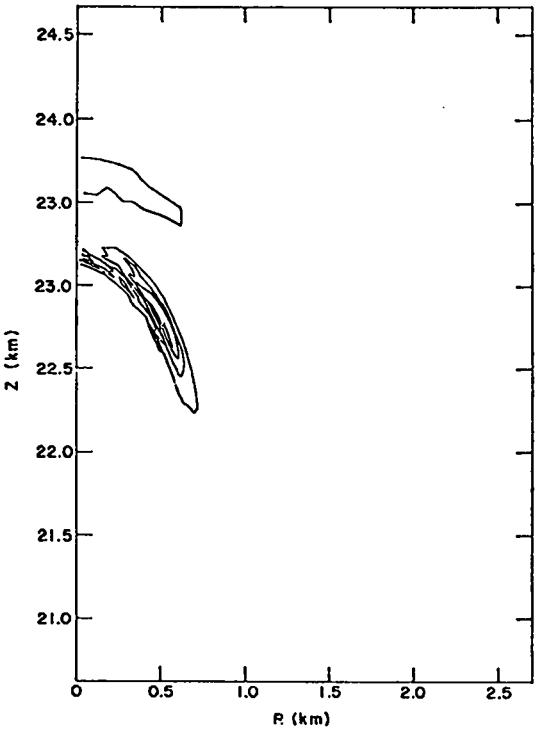


Fig. 6. Contour plots of shear creation.

Figure 6 indicates how local the shear creation, in fact, is; the same is true of the buoyancy creation. Moreover, the region of largest shear and buoyancy creation is at the upper edge of the fireball, which is also the region of steepest temperature gradients. One might expect then that the turbulence would reduce the maximum gradients and that is indeed what we find. Figure 7 shows a comparison of the maximum gradient of internal energy calculated with and without turbulence. Both of these were carried out with a fine grid and indicate what is probably the major effect of turbulence: the degrading of temperature and density gradients.

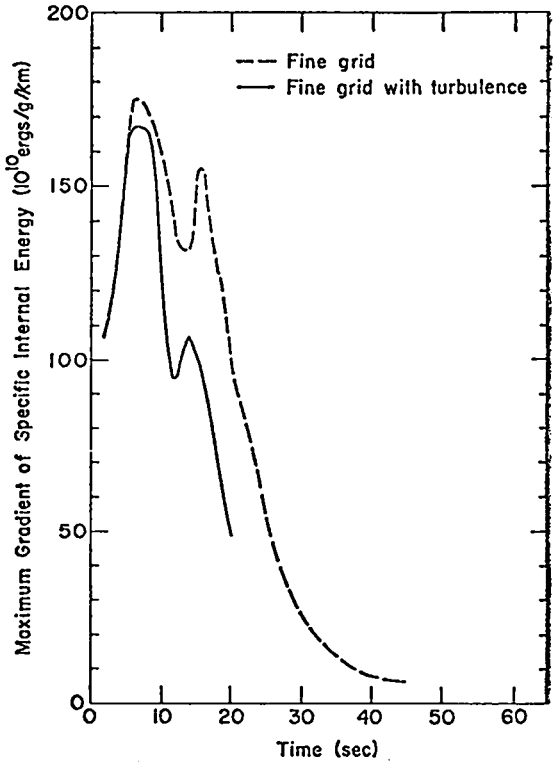


Fig. 7. Maximum gradient of internal energy with and without the inclusion of turbulence.

One can see the effect of resolution on turbulence energy by comparing contour plots from a calculation with high resolution with one of low resolution in Fig. 8. The fine grid calculation has a maximum turbulence energy 50% greater than the coarse grid result on the right. The total turbulence energy differs by about the same ratio. Since the minimum cell size in the two calculations differs by a factor of 2 1/2 and the turbulence energy by only 50%, it is reasonable to assume that further refining of the average calculation zone size will not greatly affect the level of turbulence energy. Note also that the configurations of the two calculations in Fig. 8 are similar to appearance.

Figure 9 displays a rise history for typical calculations with and without turbulence. The inclusion of the added viscosity due to turbulence causes only a slight decrease in altitude at late times. It is, however, conceivable that as better calculations with sharper gradients are performed, higher levels of turbulence may be supported, which increase the net effect. In addition, a larger value of $\beta$ would likely lead to more pronounced differences due to turbulence.

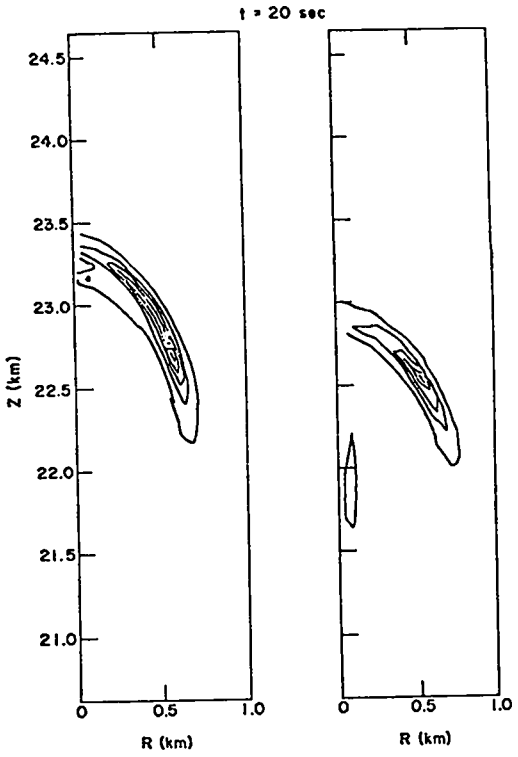


Fig. 8. Contour plots of turbulence energy for fine grid (left) and coarse grid (right) calculations.

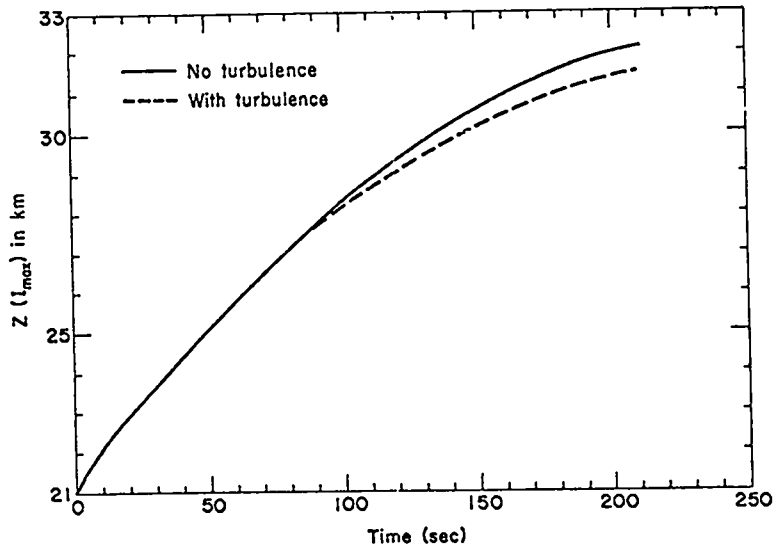


Fig. 9. Altitude as a function of time with and without the inclusion of turbulence.

Work continues in an effort to improve agreement with experiment. Several events are being studied concurrently, particularly to evaluate the agreement between the calculated and the measured radii. It appears that there are still uncertainties concerning the position of the edge of the fireball that may be resolved by a clearer interpretation of the relation between the experimental data and the numerical simulations. We also continue to refine the turbulence model and to study the sensitivity of its predictions to the parameters we include. These are just a few of the many aspects of the whole simulation effort with which we are concerned. Our primary goal remains to obtain a model that consistently predicts the dimensional behavior (rise altitude, radius, etc.) of a variety of low altitude atmospheric events.

ACKNOWLEDGMENTS

The authors are indebted to Eric M. Jones for many helpful discussions of the whole field of low altitude fireball phenomenology.

REFERENCES

1. A. A. Amsden and C. W. Hirt,"YAQUI: An Arbitrary Lagrangian-Eulerian Computer Program for Fluid Flows at All Speeds," Los Alamos Scientific Laboratory report LA-5100, March 1973.

2. C. W. Hirt, "An Arbitrary Lagrangian-Eulerian Computing Technique," Proceedings of the Second International Conference on Numerical Methods in Fluid Dynamics, Berkeley, CA (1970).

3. E. M. Jones; private communication.

4. H. M. Ruppel, R. A. Gentry, and E. M. Jones; LASL, "Calculations of Low Altitude Fireballs Using the Iced-Ale Method," presented at the DNA Low Altitude Symposium, April 1973.

5. B. J. Daly and F. H. Harlow, Phys. Fluids 13, 2634 (1970).

6. I. Wygnanski and H. Fiedler, J. Fluid Mech. 38, 577 (1969).

7. B. E. Launder, A. Morse, W. Rodi and D. B. Spalding, "The Prediction of Free Shear Flows-A Comparison of the Performance of Six Turbulence Models," Imperial College Report TM/TN/B/19 May 1972.

8. J. Laufer, NACA Report No. 1053 (1951).

## APPENDIX

NOTATION

$\rho$ = density

$\overline{\rho}$ = mean density

$\rho'$ = fluctuating density

$u_i$ = $i^{th}$ component of velocity

$\overline{u_i}$ = $i^{th}$ component of mean velocity

$u_i'$ = $i^{th}$ component of fluctuating velocity

$\rho I$ = internal energy

$\overline{\rho I}$ = mean internal energy

$\lambda$ = dilatational viscosity

$\mu$ = shear viscosity

$\delta_{ij}$ = Kronecker delta function

$\vec{X}^n_{i,j}$ = coordinate of vertex (i,j) at time level n

$\rho'I'$ = fluctuating internal energy

$t$ = time

$x_i$ = $i^{th}$ coordinate

$\sigma$ = turbulence viscosity

$s$ = internal scale

$q$ = specific turbulence energy

$g_j$ = gravitational acceleration in jth direction

$p$ = pressure

$\vec{U}^L_{i,j}$ = Lagrangian velocity of vertex (i,j)

$\langle \vec{x} \rangle$ = average value of $\vec{x}$ - coordinate of four neighbors nearest to $\vec{X}_{i,j}$